S/3 /–70

/ 40 986

Melting, Vaporization, and Energy Partitioning for Impacts on Asteroidal and Planetary Objects

P, 4

N93-19244

CATHERINE L. SMITHER AND THOMAS J. AHRENS

Lindhurst Laboratory of Experimental Geophysics,
Seismological Laboratory 252-21, California Institute of Technology

A three-dimensional smoothed particle hydrodynamics code was used to model normal and oblique impacts of silicate projectiles on asteroidal and planetary bodies. The energy of the system, initially in the kinetic energy of the impactor, is partitioned after impact into internal and kinetic energy of the impactor and the target body. These simulations show that, unlike the case of impacts onto a half-space, a significant amount of energy remains in the kinetic energy of the impacting body, as parts of it travel past the main planet and escape the system. This effect is greater for more oblique impacts, and for impacts onto the small planets. Melting and vaporization of both bodies were also examined. The amount of the target body melted was much greater in the case of smaller targets than for an impact of a similar scale on a larger body.

Smoothed particle hydrodynamics (SPH) [Monaghan & Gingold 1983, Benz at al 1986] is a technique which allows fully three-dimensional modeling of impact processes. In this study, we have used an SPH code developed at Caltech to examine the effects of impacts of silicate projectiles on planetary and asteroidal bodies to determine the extent of melting and vaporization of the impact, as well as the partitioning of energy in the system. The objects are modeled by a collection of particles, each representing a mass distribution in space, described as a function of a characteristic length scale. For each particle, the position, velocity, density, internal energy, pressure and bulk sound speed are calculated at each time step in the simulation. The system is self-gravitating, and energy and momentum are conserved throughout the run. The material properties are determined by an equation of state. For these simulations, we used the Tillotson equation of state [Tillotson 1962] for anorthosite [Ahrens & O'Keefe 1977a] for both the targets and the impactors.

We modeled impacts on two different target sizes: 1700 and 6400 km in radius, corresponding approximately to the size of the moon and the earth, respectively. Each target was hit with impactors of 40% and 60% of its radius (6% and 22% of its mass) at speeds of 10 and 20 km/s. In order to investigate the effects of oblique impacts, we varied the angle of incidence of the collision from 0° to 90°, where this angle is measured from the axis of the plane parallel to the impact trajectory to the line from the center of the target to the center of the impactor at the time of impact. Thus a normal impact corresponds to an angle of 0°, and a 90° impact is a glancing blow.

Initially, the energy of the system resides entirely in the kinetic energy of the impactor. Upon impact, some of the energy goes into ejection of material from the target, and some into heating (internal energy) of both bodies. Studies of impact onto a half-space [e.g. O'Keefe & Ahrens 1977a] show that little to none of the total energy remains in the kinetic energy of the impactor after the impact. This is as expected, since, for an impact onto a planet of effectively infinite radius, very little of the impactor material will be able to get past the target. However, for our cases of impacts on finite-sized bodies, we find that a significant portion of the total energy of the system remains in the kinetic energy of the impactor. This is especially pronounced in the more oblique, and higher velocity, collisions. Figure 1 shows the partitioning of energy for two cases of impacts on the 1700 km radius target body. The plot on the left shows the results of a 10 km/s normal impact of the smaller (40%) radius impactor. The energy is plotted normalized to the total initial energy of the system, and the time scale represents a normalized time, τ, such that $\tau = tU/r$, where U is the impact velocity, r the radius of the impactor, and t is the time in seconds. Most of the impactor is accreted to the target, so only a small fraction of the impactor material has any appreciable kinetic energy. Of the total system energy, 90% is in the internal energy of the target and the impactor. The plot on the right of figure 1 shows the results of an oblique (50°), 20 km/s collision of the larger (60%) impactor with the 1700 km target body. In this case, much of the impactor escapes the main object's gravity, and travels
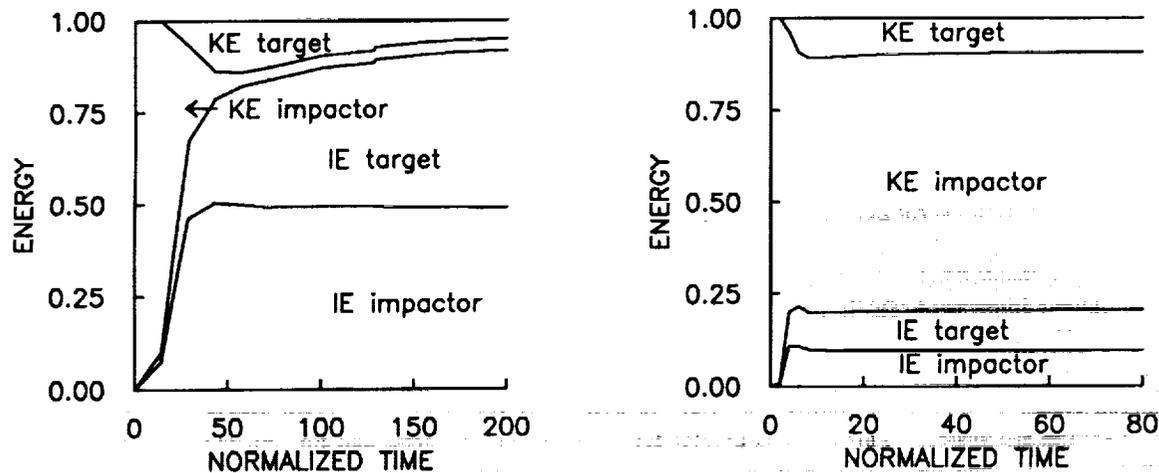
Figure 1: Partitioning of energy for two cases of impact on the 1700 km radius body. The figure on the left shows the results of a normal impact at 10 km/s with the smaller (40%) impactor. The figure on the right shows the case of an oblique (50°) collision with the larger impactor. Much of the energy of the system remains in the kinetic energy of the impactor in this case.

past it; thus, a significant amount (70%) of the total energy remains in the kinetic energy of this material. The corresponding cases for the larger target show that, in the case of a normal impact, 95% of the system energy is converted to internal energy; in the 50° impact at 20 km/s, 45% of the total energy remains in the kinetic energy of the impactor particles.

The impact causes melting of both the target and the impactor. For all but the most oblique collisions, all of the impactor is shocked to a state sufficient to cause complete melting. The smaller (1700 km) targets show much more melting than is seen in similar-sized impacts onto the 6400 km targets, as is shown in figure 2. The plots show the amount of mass of the target shocked to internal energies high enough to cause complete melting, calculated as the number of projectile masses melted, as a function of the impact angle. Normal impacts, which transfer more kinetic energy to the target, melt much more material than the oblique impacts do. The two plots show the melting of the 6400 km target (left) and the 1700 km target. The lines on each graph are labeled to identify the impact velocity in km/s and the relative size of the impactor and target (in percent). For normal and low-angle impacts, the smaller impactor melts less of the target, both in terms of the number of projectile masses and the total mass melted. The difference between the different cases is much less pronounced for more oblique impacts. Also shown in figure 2 is the amount of mass that was vaporized after the impact. The impacts onto the 6400 km target produced much more vaporization (.1 to .25 projectile masses for the 20 km/s, 40% impactor, .3 to .4 projectile masses for the 20 km/s, 60% impactor) than those onto the 1700 km targets (.1 to .2 projectile masses for the 20 km/s, 60% impactors).

The results shown above indicate that target size and impact parameter have a considerable effect on the amount of melting and vaporization and on the partitioning of energy. We also studied the formation of ejecta, material thrown off the target body at velocities greater than the escape velocity of the target, and the amount of impactor material accreted to the target. For all cases of impact onto the 6400 km body, very little material was ejected; only the 20 km/s collisions with the larger impactor were sufficient to propel material away from the target at more than the escape velocity, and the amount ejected ranged from 3 to 6% of the total mass of the target. The smaller targets lost much more mass. The larger and faster impacts at low angles were sufficient to cause catastrophic breakup of the target, where the largest fragment remaining has less than half the original mass of the target. The 10 km/s impacts with the larger impactor did not cause catastrophic breakup, but did cause 40% of the target to reach escape velocity in the case of normal impact, and 8% to escape in the 90° (glancing) impact. As was the case with the 6400 km target, collisions with the 40% impactor did not generate large quantities of ejecta. Normal impacts at 20 km/s caused 12%
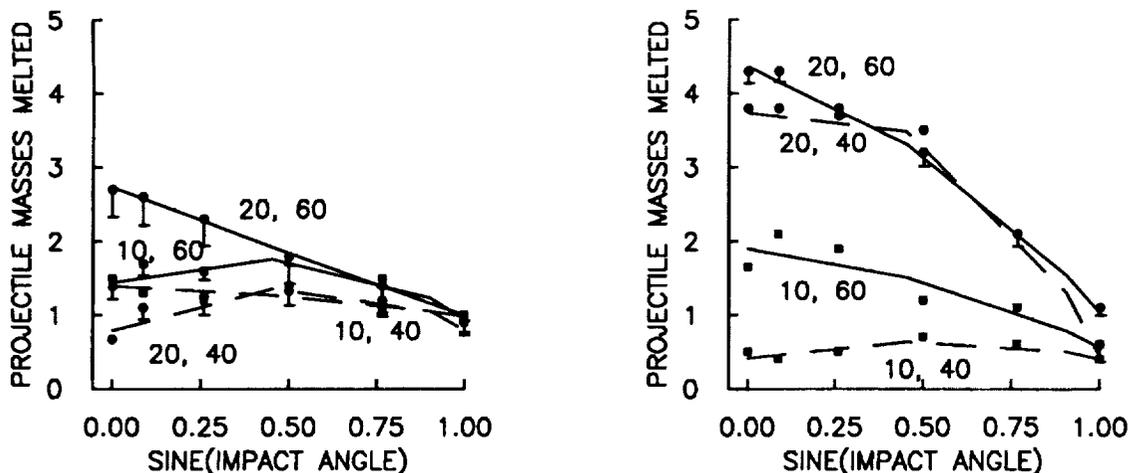
Figure 2: Melting of material on 6400 km (left) and 1700 km targets for the impacts described in the texts. The bars under some of the points show the amount of material vaporized. The smaller impacts generally show little to no vaporization. The four cases for each target are marked with two numbers, the first of which denotes the impact velocity in km/s, the second the relative size of the impactor.

of the target material to escape; 10 km/s impacts caused only 1 to 2% to escape.

For the larger targets, much of the impact mass was accreted. Except for the most oblique collisions, all of the smaller impactor remained with the target after impact. The 6400 km target, when hit by the 60% impactor at 10 km/s (a velocity lower than the escape velocity at its surface), caused 90 to 100% of the impactor material to be accreted. The only material from the impactor to escape was that which was on the side opposite the point of impact in the oblique cases. The higher velocity impacts accreted between 70 (normal impact) and 25% (90° impact) of the impactor material. The 1700 km targets, due to the lower escape velocity relative to the impact velocity, accreted much less of the impactor.

Figure 3 compares the SPH ejecta results with the two-dimensional normal-impact models of O'Keefe and Ahrens [1977b]. The curves are modified from their figure 2a, and show the amount of material, in terms of impactor masses, that reached escape velocity after impacts at 7.5, 15, 30, and 45 km/s. Our results for the two escape velocities 2.4 and 11 km/s are plotted as well. We plotted only the values from the normal and the most oblique (90°) impacts, as representative of the range of values. Only the 60% impactors are plotted, since the 40% impacts produced no measurable ejecta from the larger targets. (For this set of calculations, we cannot resolve material smaller than .018 projectile masses in the 40% case, and .005 projectile masses in the 60% case.) Our simulations of impacts of the 60% impactor produced more ejecta than predicted by the O'Keefe and Ahrens results. The normal impact onto our smaller target produced as much ejecta as would have been produced by an impact of twice the velocity onto the half-space. The ejecta predicted for the larger targets, while not as great in terms of total projectile masses as that of the smaller targets, was still much more than predicted by the half-space model. For clarity on this figure, we did not show the values for the amount of ejecta produced by the collision of the 40% impactor onto the smaller target. Normal impact caused .067 projectile masses to be ejected after the 10 km/s impact, and 2.0 projectile masses in the 20 km/s case. The corresponding values for the most oblique (90°) impact are .083 and .42 projectile masses for 10 and 20 km/s, respectively. The smaller normal impacts yield ejecta output much closer to that predicted by O'Keefe and Ahrens.

Our calculations show that the size of the target and the relative sizes of the target and the impactor are important parameters in the study of large impacts on planetary bodies. Impacts at the same specific energy (kinetic energy per unit mass) have significantly different effects on targets of different sizes. Future work will investigate this phenomenon in more detail by considering impacts onto other sizes of targets, at different velocities, for the same range of impact angles.
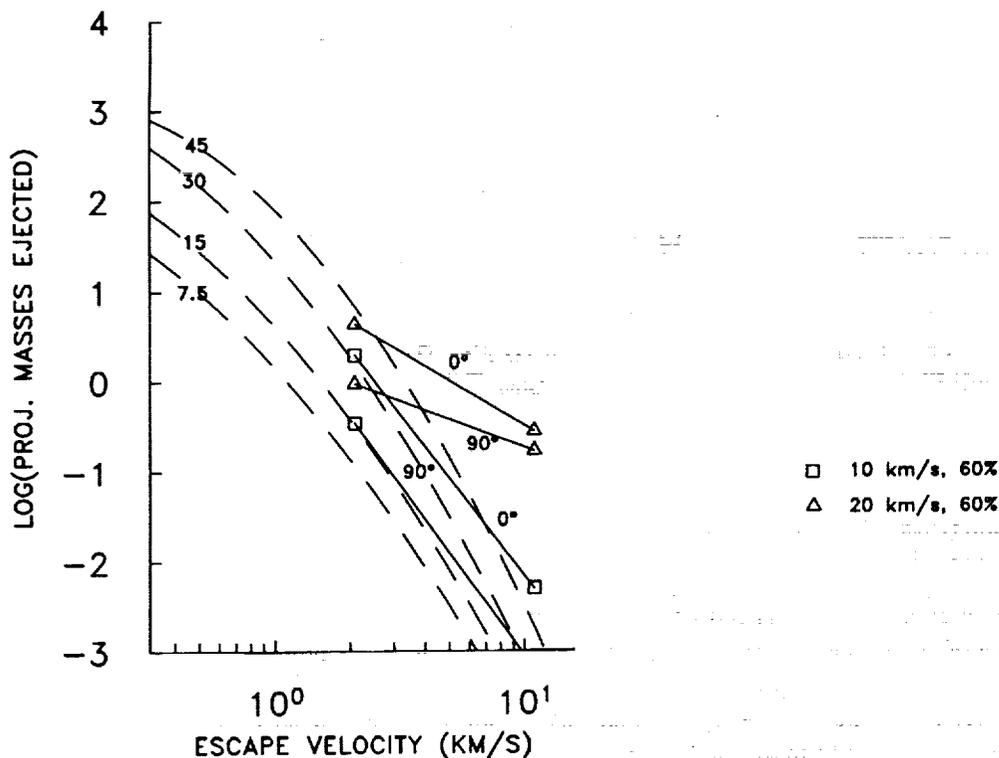
Figure 3: Mass of material ejected from the target, measured as multiples of the projectile mass. The dashed lines are modified from figure 2a of O'Keefe and Ahrens [1977b], and show the amount of ejecta produced by normal impacts at 7.5, 15, 30, and 45 km/s. The points plotted are from this study, and show the amount of ejecta from normal and glancing impacts of the larger projectile.

REFERENCES

Ahrens, T. J. and O'Keefe, J. D. Equations of state and impact-induced shock-wave attenuation on the moon, in *Impact and Explosion Cratering* 639-656 Pergamon Press, New York (1977).

Benz, W. Slattery, W. L. and Cameron A. G. W The origin of the moon and the single-impact hypothesis I, *Icarus* 66, 515-535 (1986).

Monaghan J. J. and Gingold R. A. Shock simulation by the particle method SPH, *J. Comput. Phys*, 52, 374-389 (1983).

O'Keefe J. D. and Ahrens T. J. Impact-induced energy partitioning, melting, and vaporization on terrestrial planets, *Proc. Lunar Sci. Conf. 8th*, 3357-3374 (1977a).

O'Keefe J. D. and Ahrens T. J. Meteorite impact eject: Dependence of mass and energy lost on planetary escape velocity, *Science*, 1249-1251 (1977b).

Tillotson J. H. Metallic equations of state for hypervelocity impact *General Atomic Report GA 3216* 139 pp. (1962).